Process Safety and Environmental Protection 177 (2023) 1431–1439

Contents lists available at ScienceDirect

Process Safety and Environmental Protection

journal homepage: www.journals.elsevier.com/process-safety-and-environmental-protection

Continuous boilover behaviors of large-scale kerosene pool fires under sub-atmospheric pressure

Jinlong Zhao [a], Qingyuan Zhang [a], Zhenhua Wang [a], Rui Yang [b], Jianping Zhang [c,*]

[a] China University of Mining & Technology, Beijing, Beijing 100083, China,
[b] Institute of Public Safety Research, Department of Engineering Physics, Tsinghua University, Beijing, China
[c] FireSERT, Belfast School of Architecture and the Built Environment, Ulster University, Newtownabbey BT37 0QB, United Kingdom,

ARTICLE INFO

Keywords:
Thin-layer boilover
Large-scale pool fires
Sub-atmospheric pressure, boilover intensity
Interface temperature
Thermal hazard

ABSTRACT

Accidental fire is a major safety concern in chemical parks, highlighted by the several major fire accidents involving storage tanks in recent years. Boilover is considered as one of the most destructive tank fire scenarios, which occurs when a liquid fuel burning on a water layer, leading to the explosive evaporation of water and consequently a sudden increase of the heat release rate (HRR) and associated flame height due to the splashing of burning fuel. Previous studies on boilover with large-scale pool fires were mostly conducted under normal atmospheric pressure. However, chemical parks are often located in plateau regions, where the effects of reduced pressure on boilover behaviors were rarely examined. Moreover, following the initial boilover, continuous boilover could occur, and its understanding is particularly important in the thermal hazard and risk analysis and firefighting of tank fires. In this study, thin-layer boilover experiments were conducted under sub-atmospheric pressure using aviation kerosene (RP-3) with various initial fuel thicknesses and pool diameters. The burning process, boilover intensity, temperature in the fuel and water layers and associated thermal hazard were analyzed. Experimental results showed that continuous boilover occurred in all test conditions, characterized by a high intensity initial boilover followed by a series of subsequent ones with gradually reduced intensity. The mass burning rate and flame height varied significantly during boilover. It was found that the boilover intensity increases with the initial fuel thickness but decreases with the pool diameter and approaches a nearly constant value when the pan diameter is sufficiently large. The temperature at the fuel/water interface was found to increase from 93 ℃ to around 108 ℃ during boilover, both of which are lower than those observed under normal atmospheric pressure due to reduced water boiling point. The thermal hazard calculated for the initial boilover is highest as expected, and that of subsequent boilovers gradually decreases but could still be higher than that at the steady burning stage. The findings in this work will contribute to risk assessment of continuous boilover in fire accidents.

1. Introduction

Storage tanks fires in chemical parks pose significant danger to the facility and the safety of personnel and fire fighters. Liquid fuels are prone to accidental leak during storage or transportation as highlighted by a case study that the accidental release or leak of highly flammable fuels contributed to 97% of major fire and explosion accidents (Tauseef et al., 2018). Once the released fuel from the initial accident is ignited, the resulting extreme radiation, fragments and splashing fuel could ignite the fuel vapor in adjacent tanks leading to a cascade of accidents, commonly known as the domino effect (Khan and Abbasi, 2001). The domino effect in chemical parks and, more importantly, its impact on risk assessment and management have attracted much research attention in recent years (Jiang et al., 2019; Ding et al., 2021; Ding and Ji, 2023; Sun et al., 2022). The accident consequence of benzene leakage from storage tank (Zhou et al., 2023) and large-scale pool fires in oil storage (Ahmadi et al., 2019a) were also assessed using Areal Location of Hazardous Atmospheres (ALOHA) and a computational fluid dynamics (CFD) model respectively.

There are many cities in the world located in plateau regions, such as Brasilia, the capital of Brazil (altitude: 1158 m) (Hua, 2011). In recent decades, the number of chemical parks has increased rapidly in these

* Corresponding author.
E-mail address: j.zhang@ulster.ac.uk (J. Zhang).

https://doi.org/10.1016/j.psep.2023.07.086
Received 6 June 2023; Received in revised form 17 July 2023; Accepted 28 July 2023
Available online 2 August 2023

regions with the development of plateau economy. Once the accidentally released fuel is ignited and, if not controlled immediately, the fire can spread quickly to cover the whole fuel surface. During fire rescue, the fire extinguishing agent contains a large amount of water, leading to a particular fire scenario, i.e., a thin-layer of fuel burning on a water surface, which is the primary focus of this study. When boilover occurs, it can result in a significant change in the mass burning rate and flame height and associated thermal hazard, posing a greater threat to the surrounding equipment and firefighters (Shaluf and Abdullah, 2011; Ahmadi et al., 2019b). Furthermore, continuous boilover may occur after the initial boilover, and its understanding is important for fire rescue. For example, a storage tank fire accident occurred at a chemical park in Ningxia with four fatalities. The leaked fuel floated on the water layer and continuous boilover occurred, resulting in great difficulties in firefighting. In plateau regions, air pressure is low and both the boiling points of water and liquid fuel decrease, which could further affect the thin-layer boilover process as demonstrated in Hu et al. (2011). It is, therefore, of great practical importance to study the boilover behaviors of thin-layer fuels under sub-atmospheric pressure conditions and to characterize the resulting thermal hazard, which in turn can help improve the targeted firefighting strategy for tank fire accidents.

Significant research has been conducted to investigate boilover behaviors, occurrence mechanism and thermal hazard under normal atmospheric pressure. Fan et al. (1995) observed that the flame height and liquid layer temperature increased during boilover and divided the burning process into three periods: quasi-steady, boilover premonitory and boilover. Laboureur et al., (2012, 2013) reported using a mixture of diesel and oil that the bubbles appearing at the fuel/water interface are an essential condition for boilover. Broeckmann et al. (1995)) found that a thin boiling layer with stable temperature was formed under the fuel surface during burning and also suggested that the water at the water/fuel interface reaching its boiling point was an essential condition for boilover occurrence. Koseki et al. (2006) found using Arabian light crude oil that the ratio of the mass burning rate at the boilover stage to that at the quasi-stable stage (boilover intensity) increases with fuel thickness. Garo et al. (1994) performed experiments using heating oil and found that the onset time and intensity of boilover increased with the increase of initial fuel layer thickness whilst decreasing with an increase of pan diameter. Kong et al. (2017) experimentally studied the boilover phenomenon of crude oil in open conditions and developed, based on mass burning rate and flame height measurements, a model for estimating the boilover intensity. Ferrero et al. (2007) carried out experiments using a thin-layer of diesel-oil on a water layer and proposed that an increase of safety distance is needed in the case of thin-layer boilover accidents due to an increase of heat release rate and flame height during boilover. More recently, Kong et al. (2021) conducted experiments using crude oil with different pan diameters and initial fuel thicknesses to explore the hazardous characteristics of boilover splash and proposed a model for the safety distance based on the boilover splash coverage ratio by analyzing the relationship between boilover splash and a dimensionless distance.

Due to the increasing number of chemical parks built in plateau regions, boilover behaviors of liquid fuels under sub-atmospheric pressure have also been studied by several researchers, albeit in small-scale. Lin (2017) conducted experiments (D: 0.15–0.4 m) using thin-layer fuels under different pressures (64–101 kPa) and found that, with a decrease of pressure, the temperature at the fuel/water interface decreased. Ma (2020) performed experiments (D: 0.15–0.4 m) using kerosene and diesel under three different pressures (64, 76, 101 kPa) and reported that both the mass loss rate and boilover intensity decreased under sub-atmospheric pressure. Chen et al. (2018) carried out experiments (D: 0.15, 0.18 m) in Hefei (100.8 kPa) and Lhasa (64 kPa) and used sound intensity to characterize the boilover intensity and observed a positive correlation between pressure and boilover intensity.

The above studies have clearly shown that boilover behaviors of liquid fuels can be affected by a large number of parameters such as fuel type, initial fuel thickness, pool diameter and pressure. Experimental data under sub-atmospheric pressure is still limited, especially concerning large-scale experiments. Furthermore, previous studies focused mostly on the first (initial) boilover and less attention was paid to the subsequent continuous boilover, which could have a great impact on thermal hazard and risks analysis and needs further investigating. In this work, large-scale boilover experiments using a thin-layer of aviation kerosene (RP-3) were carried out under sub-atmospheric pressure. The initial fuel thickness and pan diameter were varied to examine their respective effects on boilover characteristics, including boilover intensity, burning rate, flame height and temperature evolution inside the liquid layer (fuel and water). The continuous boilover behaviors and the corresponding thermal hazard were also examined.

2. Experimental details

The overall schematic of the experimental setup is shown in Fig. 1. Two types of fuel pans, made of stainless steel (3 mm thick), were used: (a) circular pans with diameters of 40, 80 and 120 cm and a side wall height of 20 cm and (b) a square pan with a side length (L) of 2.5 m (equivalent diameter of 2.8 m), and a side wall height of 40 cm. The reason for using a square pan for the largest diameter is the design of the pan, which was comprised of several small parts for easy transportation and assembly. For large-scale pool fires, the experiment results obtained using square or circular pans (with the same fuel surface area) are expected to be almost the same because of strong air entrainment at the flame base and the resulting flame/fire plume being axisymmetric. For the experiments with the circular pans, the pan was placed on the top of a load cell (maximum: 35 kg; precision: 0.1 g) to record the real time mass loss of the fuel, based on which the burning rate was calculated. For the experiments with the square pan, the communicating vessels principle was used to calculate the burning rate (Liu et al., 2021).

A CCD camera and an infrared camera were used to record the flame contour and flame temperature respectively. They were positioned at 10 m horizontally away from the pool center at a height of 1.5 m. The flame images by the CCD camera at a frequency of 25 fps were used to calculate the mean flame height via image processing (Hu et al., 2012; Chen et al., 2022). In order to simulate the boilover fire, water (10 cm) was injected into the pan before fuel was added. Three initial fuel thicknesses were used: 10, 15, and 20 mm. A set of 7 K-type thermocouples (bead diameter: 1 mm; maximum: 1200 K) was positioned evenly inside the pan at a 5 mm interval to measure the temperature of the liquid fuel and water. The first thermocouple was 9 cm from the pan bottom surface as shown in Fig. 1(b). They were numbered 1–7 from bottom to top. A water-cooled heat flux meter (SGB 01, with a measurement range of 50 kW/m^2 and a view angle of 180°) was positioned at three times of the pool diameter from the pool center (3D) and 1 m above the ground to measure the radiative heat flux. Aviation kerosene (RP-3) with a purity of more than 99% was used as the fuel and its detailed thermal properties are shown in Table 1.

The experiments were carried out in an outdoor environment in Qinghai Province (atmospheric pressure: 69 kPa). A windproof net was installed around the experimental setup to reduce the impact of wind. The wind speed inside the windproof net was less than 1 m/s during the experiments, which was confirmed to have no impact on the experiments (Chatris et al., 2001). A total of 12 test conditions were examined as shown in Table 2. Each test condition was repeated three times to ensure the reliability of the experiments.

3. Results and discussion

3.1. Burning process

The whole burning process of thin-layer boilover is shown in Fig. 2, using Test 6 as an example. After the ignition, the flame spread rapidly to the entire fuel surface. The mass burning rate and flame height

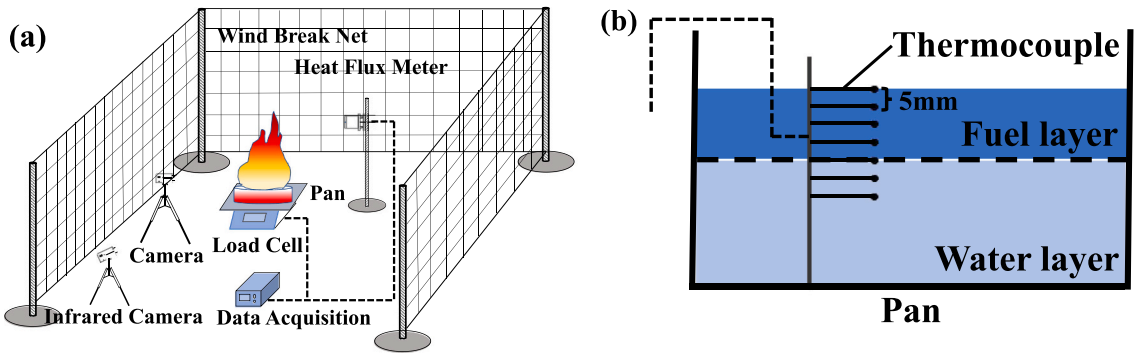

Fig. 1. The schematic of experimental setup and detail layout of thermocouples.

Table 1
Thermal properties of RP-3 kerosene (Wang et al., 2022).

Properties	Value
Flash point (℃)	60
Density (kg/m^3)	795
Boiling point and range (℃)	130–300
Heat of combustion (kJ/kg)	42800

Table 2
Specifications of the test conditions.

No.	Pan diameter D (cm)	Initial fuel layer thickness h_0 (mm)	No.	Pan diameter D (cm)	Initial fuel layer thickness h_0 (mm)
1	40	10	7	120	10
2	40	15	8	120	15
3	40	20	9	120	20
4	80	10	10	280	10
5	80	15	11	280	15
6	80	20	12	280	20

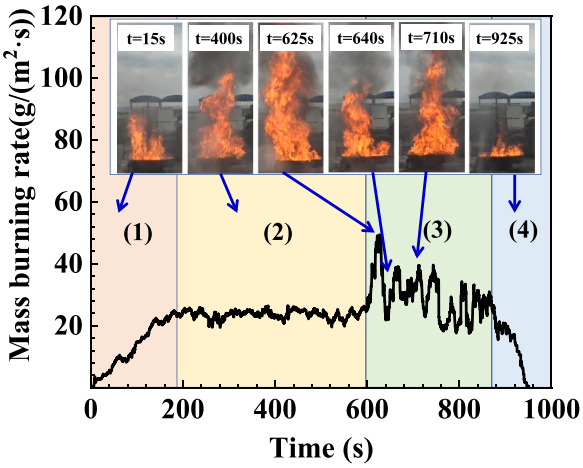

Fig. 2. The whole burning process vs. time (D:80 cm; h_0:20 mm).

continued to increase, followed by a relatively long steady burning period. As the fuel was being consumed, both the burning rate and flame height suddenly increased sharply, accompanied by crackling noises, indicating the onset of boilover. After the initial boilover, both the burning rate and flame height decreased substantially and became similar to those before boilover. However, as burning continued, both increased again, followed by a series of continuous boilover during the whole burning process and finally extinction occurred after all fuel was consumed. Based on the variations of the mass burning rate and flame height, the whole burning process can be divided into four phases: (1) initial burning; (2) steady burning; (3) continuous boilover; (4) extinguishing, which are consistent with those at normal atmospheric pressure (Zhao et al., 2020). It is worth noting that a similar burning process was also observed in the other tests.

To understand the occurrence of boilover, it is important to examine the heat transfer process as shown in Fig. 3. The heat balance of the liquid layer can be described as (Vali et al., 2014):

$$\dot{q}_{cond} + \dot{q}_{conv} + \dot{q}_{rad} = \dot{q}_{fuel} + \dot{q}_{loss} \quad (1)$$

where $\dot{q}_{cond}$ is the conduction from the pan sidewall to the liquid layer; $\dot{q}_{conv}$ is the convective heat transfer between the flame and fuel surface; $\dot{q}_{rad}$ is the flame radiative heat feedback; $\dot{q}_{fuel}$ is the heat absorbed by the fuel layer; and $\dot{q}_{loss}$ represents the heat loss to the surroundings.

Note that $\dot{q}_{fuel}$ contains two parts (Hamins et al., 1994): $\dot{q}_{preheat}$, the heat needed to raise the temperature of the fuel to its boiling point ($\dot{q}_{preheat} = \dot{m}'' C_p (T_b - T_0)$, where $\dot{m}''$ is the mass burning rate; C_p is the average specific heat capacity; T_b and T_0 are the boiling point and the initial temperature of liquid fuel, respectively) and $\dot{q}_{evap}$, the heat needed for fuel vaporization. The heat loss term $\dot{q}_{loss}$ includes the radiation partly reflected at the fuel surface ($\dot{q}_{ref}$), which is usually neglected in

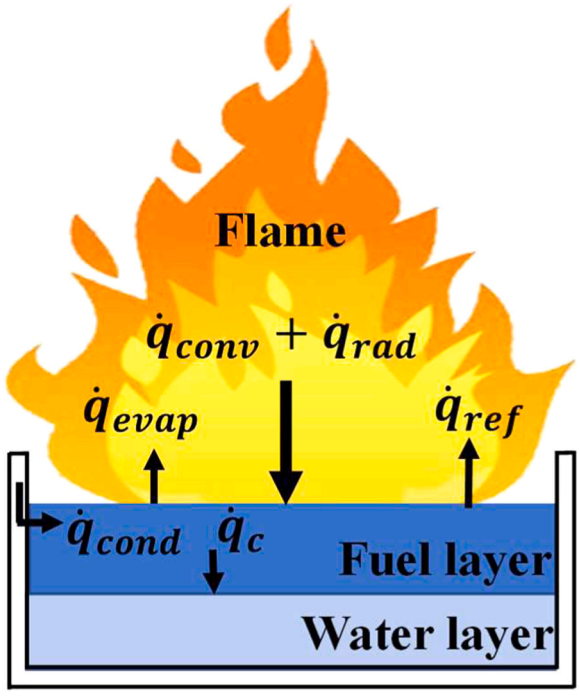

Fig. 3. The heat transfer mechanism in the liquid layer in pool fire.

pool fires, and the heat conduction from the fuel layer to the water layer ($\dot{q}_c$), which is the main heat transfer mechanism responsible for increasing the temperature at the fuel/water interface and ultimately the onset of boilover.

Fig. 4 presents the temperature histories at different depths for Test 6. During the initial burning stage, the fuel temperature at all locations increased quickly, due to an increase of flame height and radiative heat feedback from the flame to the fuel surface. At 10 mm below the fuel surface, temperature reached 190 ℃ at 370 s, and then remained constant for some time. This indicates that there was a boiling layer below the fuel surface, which is consistent with the finding in Vali et al. (2014). This temperature (190 ℃) is slightly lower than that reported (198 ℃) under normal atmospheric pressure (Ding, 2016). The temperature at the fuel/water interface reached the boiling point (93 ℃) at around 610 s, after which boilover occurred. The slightly lower boiling temperature was because water was more prone to boiling under sub-atmospheric pressure (Chen et al., 2018). It can be noted that the temperature measured at the fuel/water interface (93 ℃) was slightly higher than the water boiling point (90 ℃) at this pressure. This can be attributed to the disturbance at the fuel-water interface prior to boilover and the pressure increase caused by the fuel layer above the interface. Following the initial boilover, the temperature at the fuel/water interface fluctuated around 93 ℃ during the continuous boilover stage.

3.2. Boilover intensity

3.2.1. Initial boilover intensity

The boilover intensity is commonly defined as the ratio of the maximum mass burning rate during the boilover stage to the steady mass burning rate (Koseki et al., 2006). However, because of the uncertainties in determining accurately the maximum mass burning rate due to large fluctuations, the averaged mass burning rate during the boilover period can be used to replace the maximum mass burning rate (Kong et al., 2021; Ferrero et al., 2006), so the boilover intensity can be calculated as:

$$I_{b,a} = \frac{\dot{m}_{b,a}}{\dot{m}_s} \tag{2}$$

where $\dot{m}_{b,a}$ is the average mass burning rate at the boilover stage, g/(m^2·s) and $\dot{m}_s$ is the mass burning rate at the steady stage, g/(m^2·s).

It should be noted that, after boilover, the mass burning rate doesn't represent the fuel burning rate as it also consists of the evaporation of water and splashing fuel droplets. However, it is not possible to differentiate their contributions due to the highly transient nature of the burning process during flashover. The mass burning rate is thus used only to characterize the boilover intensity.

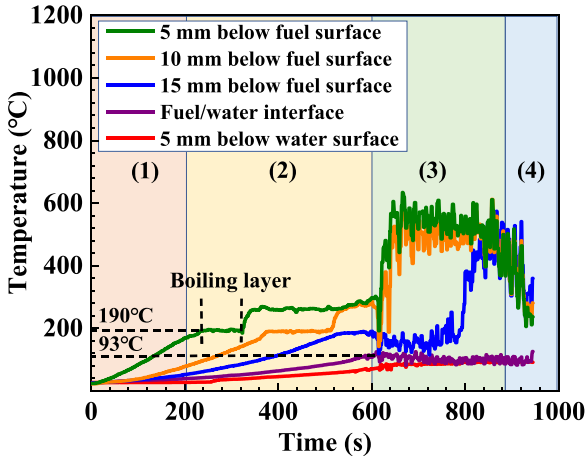

Fig. 4. Temperature histories in the fuel and water layers (D:80 cm; h_0:20 mm).

To demonstrate the effects of initial fuel layer thickness and pan diameter on the boilover intensity, Fig. 5 presents the boilover intensity of the initial boilover as a function of initial fuel layer thickness for different pan diameters. The initial boilover intensity increases with the increase of initial fuel layer thickness, which is consistent with that found at normal atmospheric pressure (Kong et al., 2017). This can be explained by noting that with a larger initial fuel layer thickness, the fuel layer at boilover is thicker and the pressure at the fuel/water interface is greater, which would result in larger bubbles when boilover occurs (Ferrero et al., 2006). Furthermore, with a larger fuel layer thickness, the heating of the water vapor by the high-temperature fuel layer becomes more significant.

Fig. 5 also indicates that the initial boilover intensity decreases as the pan diameter increases. This can be attributed to the fact that, as the pan diameter is increased, the burning rate increases and there is less fuel remaining when boilover occurs (Ferrero et al., 2006). Interestingly, with an increase of the pan diameter, the increasing rate of the initial boilover intensity decreases gradually and becomes nearly one for the case with the largest pan diameter. This is because the heat transfer from side walls is important for small-scale pool fires and fuel temperature is high. In comparison, for large-scale pool fires, radiative heat feedback is the dominating heat transfer mode and the conductive heat transfer from side walls to the liquid layer can often be ignored and, as a result, the burning rate is relatively close, and the corresponding fuel layer thickness is almost the same when boilover occurs (Heskestad et al., 1998).

In order to characterize the relation between the initial boilover intensity and the fuel layer thickness and pan diameter, Chatris et al. (2001) introduced a parameter Λ (the ratio of the initial fuel layer thickness to the fuel surface area, mm/m^2) and reported that (i) the boilover intensity increases with Λ and (ii) there is a limiting value of Λ, below which no increase in the burning rate was observed. In Fig. 6, we plot the calculated initial boilover intensity against Λ for all test conditions. For comparison, the data of thin-layer kerosene at normal atmospheric pressure (Lin, 2017) is also included. The trends of the present results are consistent with these reported in Laboureur et al. (2013). The boilover intensity can be positively correlated with Λ and approaches one when Λ is very small, confirming that the pan diameter has limited effect on the boilover intensity for large-scale burning of thin-layer fuels.

The boilover intensity under sub-atmospheric pressure appears slightly lower than that under normal atmospheric pressure, although more data for normal atmospheric pressure would be needed to confirm

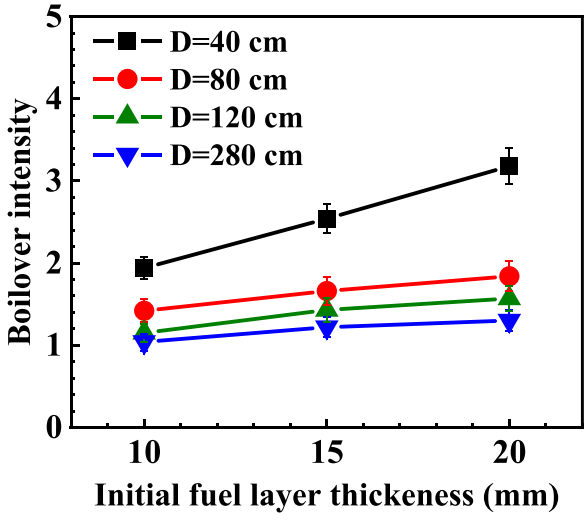

Fig. 5. The initial boilover intensity as a function of initial fuel layer thickness for different pan diameters.

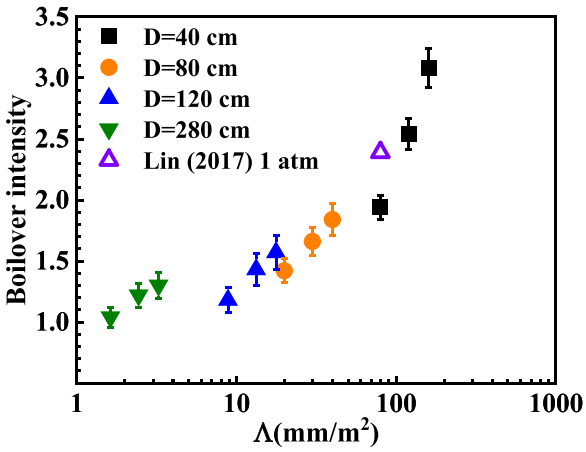

Fig. 6. The initial boilover intensity evolution with Λ, the ratio of the initial fuel layer thickness to the fuel surface area.

this. One likely explanation is that the boiling points of both fuel and water are reduced under sub-atmospheric pressure, as verified by the temperature measurements in Fig. 2 and there are fewer water vapor bubbles at the fuel/water interface and the heating effect of the fuel layer on water vapor is also reduced (Lin, 2017).

3.2.2. Continuous boilover intensity

In addition to the initial boilover, subsequent boilovers can also create significant thermal hazard during firefighting. Fig. 7 shows the variation of the boilover intensity as a function of the number of boilover. It is worth noting that only the first five boilovers are shown here, even though more were observed in some of the tests. The continuous boilover intensity decreases gradually with the number of boilover, in that the fuel was being constantly consumed and ejected when boilover occurred. After the occurrence of each boilover, the residual fuel mass was less and the pressure at the fuel/water interface became lower, resulting in a reduction of the boilover intensity. There is relatively more difference between the cases with h= 10 mm and h= 15 mm, which could be explained by the fact that for a small fuel thickness (i) there is less fuel available for boilover and (ii) it also takes a shorter time to reaching boilover, so less heat has been transferred to the water layer. As also shown in Fig. 7, for the cases with large pan diameters (120 and 280 cm), the boilover intensity of subsequent boilovers is lower than that observed with small pan diameters, which is consistent with the variation of the initial boilover with pan diameter shown in Fig. 5.

3.3. Temperature evolution during boilover

As the boilover process is closely related to the liquid layer temperature, Fig. 8 shows a comparison of the average liquid temperature at different depths before and after the initial boilover for Tests 5 and 9. It can be seen that the temperature at the fuel/water interface is around 93 ℃ before the initial boilover. The temperature at the interface

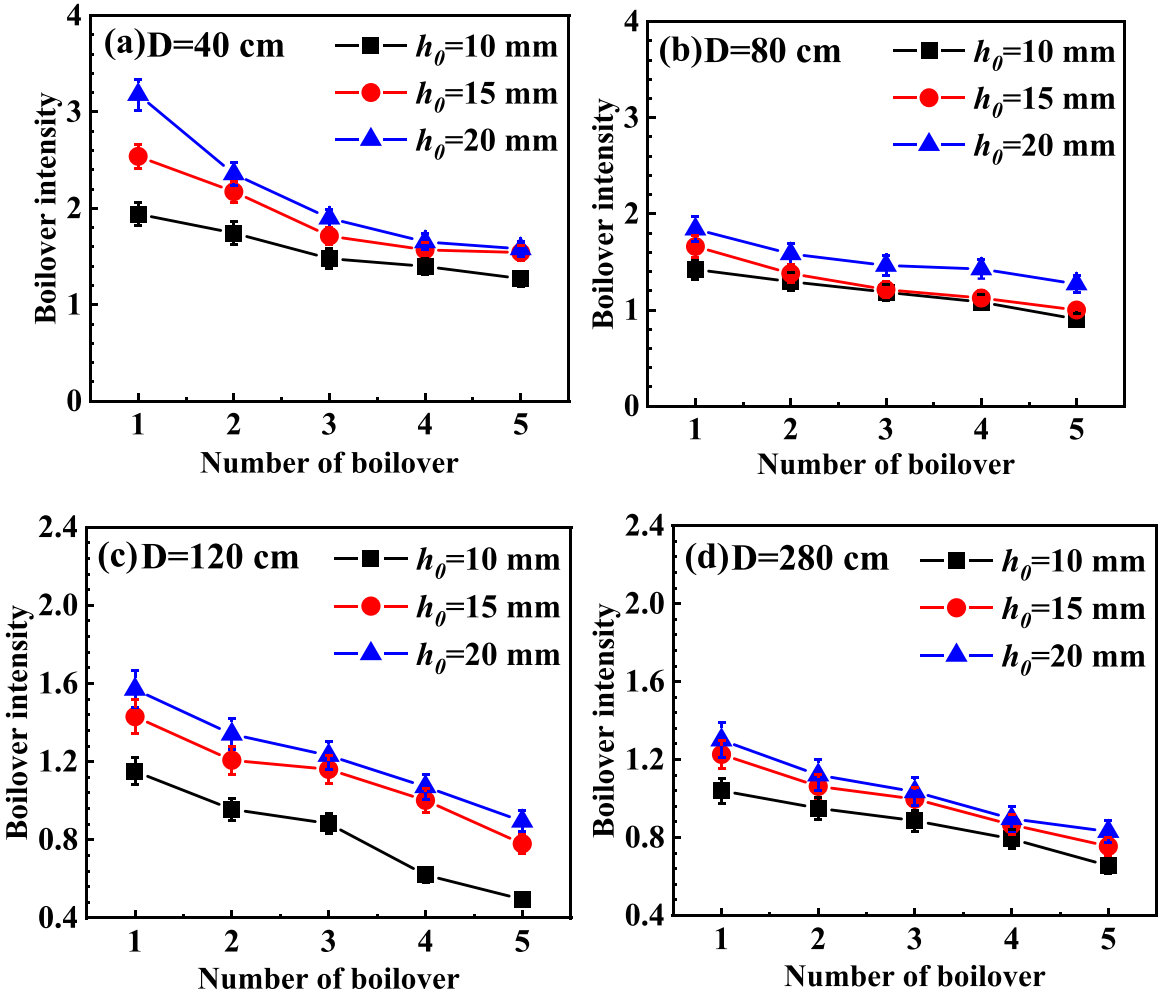

Fig. 7. The evolution of boilover intensity a) D= 40 cm; b) D= 80 cm; c) D= 120 cm; d) D= 280 cm.

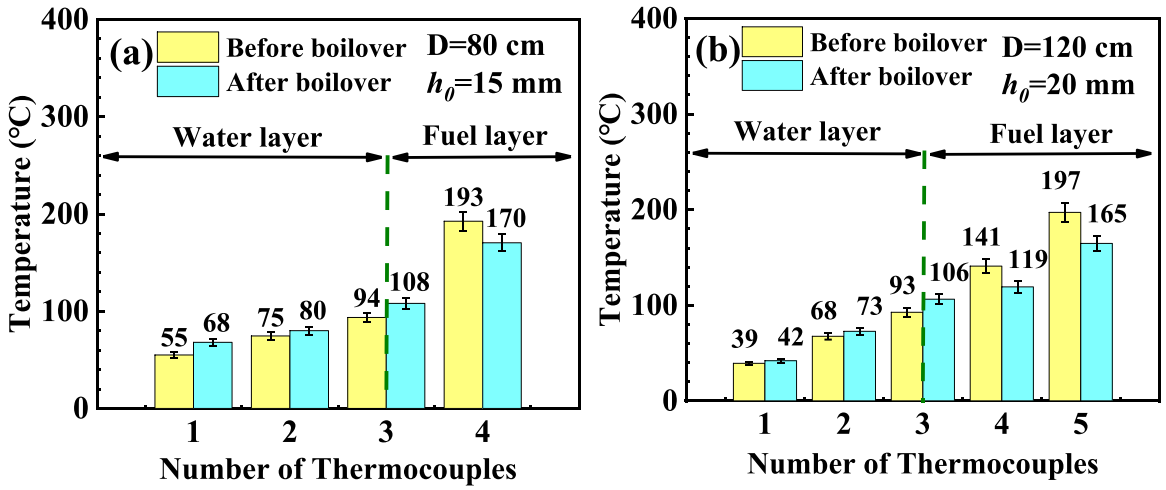

Fig. 8. The measured liquid temperature evolution during initial boilover (No. 1 TC is 10 mm below the interface; No. 2 TC is 5 mm below the interface; No. 3 TC is at the interface; No. 4 TC is 5 mm above the interface; No. 5 TC is 10 mm above the interface): a) D:80 cm, h_0:15 mm; b) D:120 cm, h_0:20 mm.

increases after boilover, reaching around 108 ℃. Both temperatures are lower than those reported under normal atmospheric pressure by Garo et al. (1994), where it was shown that the temperature at the fuel/water interface is around 100 ℃ before boilover and then increases to 120 ℃ after boilover. The difference is mainly because the water boiling point decreases under sub-atmospheric pressure and the pressure at the fuel/water interface also decreases. Fig. 8 also shows that after the initial boilover, the temperature of the water layer increases rapidly, while that of the fuel layer drops suddenly. This indicates that boilover destroyed the boiling layer at the surface of the burning fuel, which in turn led to the decrease of the burning rate and flame height after boilover as observed in the experiments.

To further understand the effects of boilover on the temperature of the liquid layer in the continuous boilover stage, a comparison of the

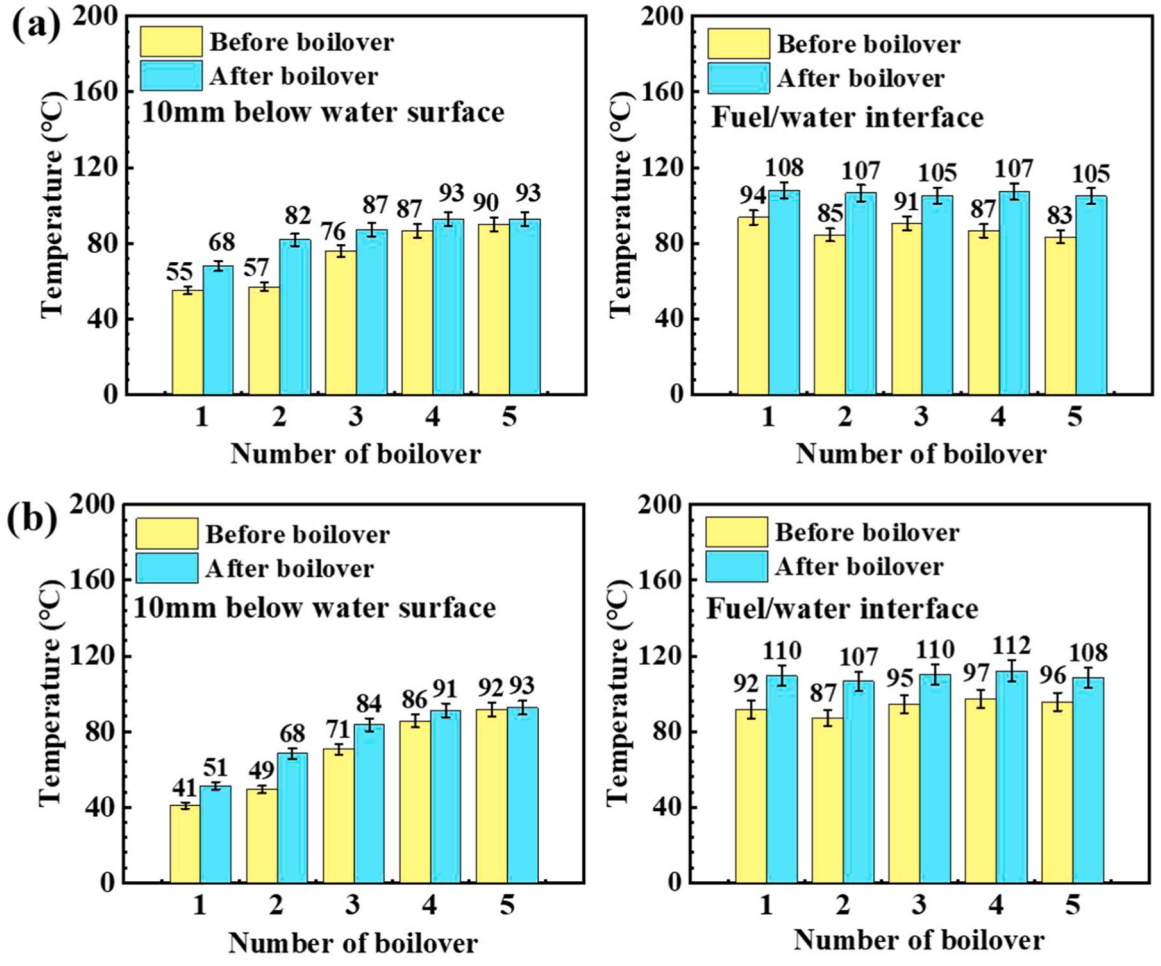

Fig. 9. The measured liquid temperature variation during continuous boilover a) D:80 cm, h_0:15 mm; b) D:280 cm, h_0:15 mm.

temperature of the liquid layer before and after the first five boilovers is shown in Fig. 9. The temperature at the fuel/water interface increases noticeably from the water boiling point to above 100 ℃ during each boilover. This is because a large number of bubbles were generated at the fuel/water interface when boilover occurred, which were heated continuously by the high-temperature fuel layer (Laboureur et al., 2013; Garo et al., 1994). After boilover, the bubbles disappeared and the temperature at the fuel/water interface returned to the water boiling point. The temperature variation at the interface appears smaller for the cases with large pan diameters. This could be attributed to the reduced boilover intensity for these cases as shown in Fig. 7 and reduced heat transfer between the fuel and water layers. The temperature of the water layer rises continuously when boilover occurs. However, the rising rate decreases gradually with the number of boilover until the temperature becomes nearly the same as the water boiling point. Results also show that with the increase of the number of boilover, there is a boiling layer below the fuel/water interface because of the continuous heat and mass transfer between the fuel and water layers, which also explains why the time interval of multiple boilovers was gradually shortened.

3.4. Thermal hazard assessment

For thermal hazard assessment of liquid fuel fires, the solid flame radiation model is widely used to calculate the radiative distribution from the flame (Hankinson and Lowesmith, 2012; Li and Zhang, 2021). In this model, the flame is assumed to be a vertical cylinder emitting thermal radiation from its surface and consists of two separate flames, one above the target and one below, as shown in Fig. 10.

The radiative heat flux can be expressed as:

$$q^{''} = E_f F \tau \tag{3}$$

where E_f is the flame surface emissive power, which is closely related to flame temperature; F is a view factor, which is related to the flame shape and the distance between the flame and the object; τ is the atmospheric transmissivity, approximated as one when approaching the target (Sudheer and Prabhu, 2010).

For the flame surface emissive power , McGrattan et al. proposed the following correlation (McGrattan et al., 2000):

$$E_f = \sigma \varepsilon_f T_f^4 \tag{4}$$

$$\varepsilon_f = 1 - e^{-k'D} \tag{5}$$

where σ is the Stefan−Boltzmann constant; T_f is the flame temperature, K; k′ is a constant, which equals the extinction coefficient multiplied by the mean beam length corrector ($k\beta$) and a value of 0.65 is used in this work (Wang et al., 2022).

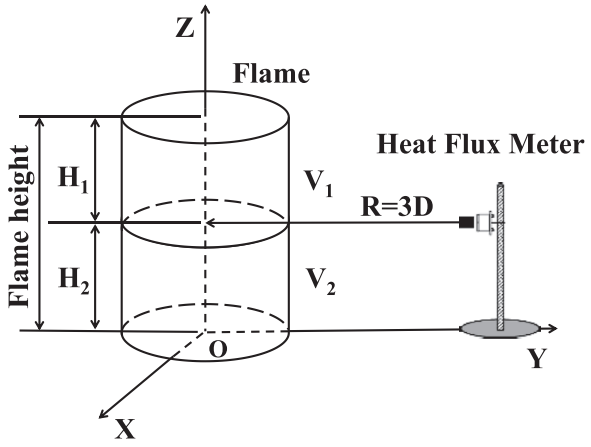

Fig. 10. The schematic of heat radiation transfer process between flame and heat flux meter.

For the flame temperature, an average value of 690 ℃ was used, as it was observed that the variation of flame temperature during the boilover stage is relatively small. It should be noted that whilst the flame surface emissive power during boilover is assumed to be constant, the flame height varies not only between different tests but also during the multiple boilovers.

The view factor between the flame and the target was calculated using the method proposed by Mudan (1984) for two cylindrical flames (see Appendix A for more detail). Fig. 11 presents the variation of the measured flame height and calculated view factor as a function of the number of boilover for Test 11 (D:280 cm, h_0:15 mm). The flame height increases when the initial boilover occurs, but as burning continuous, the flame height gradually decreases until it becomes smaller than that at the steady stage. The evolution of the view factor is similar to that of the flame height. At the initial boilover, the view factor increases from the steady stage value of 0.096–0.105, resulting in an increase in the calculated radiative heat flux from 4.49 to 5.01 kW/m^2. As expected the thermal hazard of the initial boilover is higher than that at the steady stage, but that due to continuous boilover decreases gradually. For practical thin-layer boilover fires, the burning scale is often large. Based on the variation of the burning rate and flame radiation, it can be noted that the strengthening effect of boilover on thermal hazard at the continuous boilover stage gradually diminishes with the increase of pan diameter. It should be emphasized though that as the steady burning rate and flame radiation of large-scale fires are much higher than those in smaller scale, they would still pose a greater thermal hazard at the continuous boilover stage even their boilover intensity is reduced. Moreover, the boilover interval shortens for large-scale boilover, indicating the reduction of relative safety time between two adjacent boilovers, the understanding of which is important for the safety of firefighters.

Fig. 12 shows a comparison of the calculated and measured heat flux at both steady and continuous boilover stages. The two sets of data are in good agreement with a maximum relative difference less than 20%, which verifies that the flame radiation model can be used to estimate the radiation impact on adjacent objects or personnel. Such information is important in firefighting and rescue, especially in the selection of firefighting equipment and consideration of safety distance during firefighting.

4. Conclusions

In this work, large-scale boilover experiments with a thin-layer of kerosene on a water surface were carried out under sub-atmospheric pressure. The effects of initial fuel thickness and pan diameter on boilover intensity were examined. The continuous boilover behaviors and corresponding thermal hazard were investigated and analyzed. The main findings are as follows:

(1) For burning of thin-layer fuels on a water surface, the whole burning process can be divided into four stages: initial burning, steady burning, continuous boilover and extinguishing stage. Both the mass burning rate and flame height increased significantly during the initial boilover, after which both decreased substantially, characterized by weak burning and reduced temperature of the fuel layer. This was attributed to the destruction of the boiling layer, which was also observed in subsequent boilovers. Under sub-atmospheric pressure (69 kPa), the temperature at the fuel/water interface increased from 93 ℃ to around 108 ℃ during boilover, both of which are less than those reported at normal atmospheric pressure because of the reduced water boiling point under sub-atmospheric pressure.

(2) The boilover intensity increased with the increase of initial fuel thickness but decreased with increasing pan diameter and approached a nearly constant value when the pan diameter is sufficiently large, indicating that pan diameter has limited effect on boilover intensity for large-scale burning of thin-layer fuels. During the continuous boilover

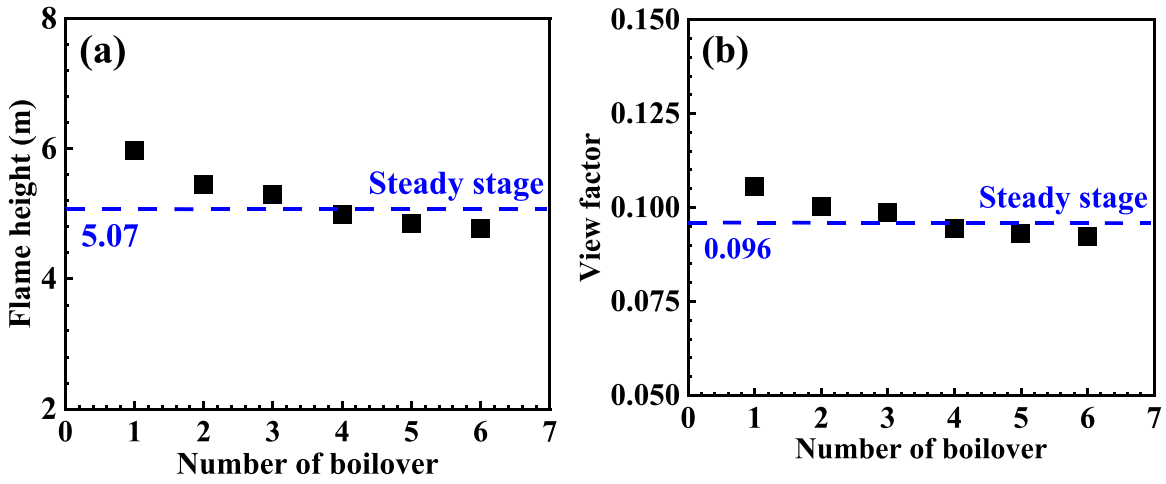

Fig. 11. a) The flame height vs. boilover time; b) The view factor vs. boilover time (D:280 cm, h_0:15 mm).

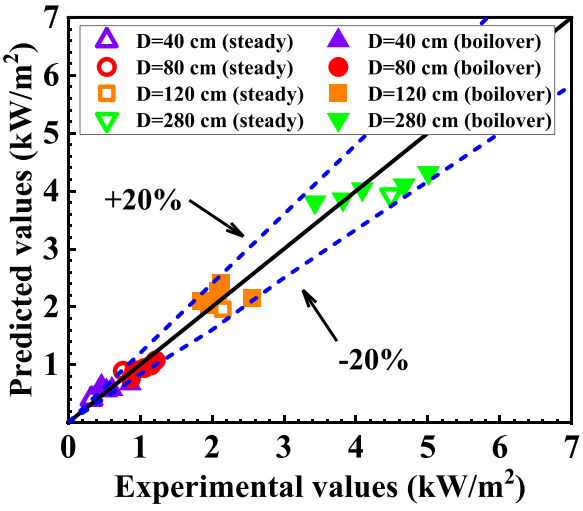

Fig. 12. Comparison of calculated and experimental radiative heat flux at steady and continuous boilover stages.

stage, the boilover intensity decreased as the number of boilover increases and the intervals between them gradually shortened.

(3) As expected, the thermal hazard for the first few boilovers was larger than that of steady burning. However, as burning continued, the calculated thermal hazard gradually decreased until eventually becoming lower than that at the steady burning stage. It is worth pointing out that, although the boilover intensity is smaller for large pan diameters, the thermal hazard in these cases remains much higher than those in small pan diameters due to increasing burning rate and flame height. Thus, the threat of thermal hazard during continuous boilover on surrounding facilities and firefighters cannot be ignored in practical scenarios. In addition to thermal hazard, close attention should also be paid to the influence of the continuous boilover period on fire extinguishing strategies and potential harm to personnel due to splashing fuel. The findings from boilover phenomena and thermal hazard analysis also provide guidance on safety protection during fire rescue.

The present data clearly highlighted the importance of the burning and continuous boilover behaviors of thin-layer fuels on a water surface under sub-atmospheric pressure conditions. More tests will be conducted in our future work with other fuels and different pan diameters and pressure conditions for further validation of the model proposed in this work for thermal hazard assessment.

Declaration of Competing Interest

The authors declare that they have no known competing financial interests or personal relationships that could have appeared to influence the work reported in this paper.

Acknowledgements

This work was supported by the Key Research and Development Program of National Fire and Rescue Administration (No. 2022XFZD04) and the Fundamental Research Funds for the Central Universities (No. 2020QN05).

Appendix A

The flame is divided into V_1 and V_2 parts (see in Fig. 10) and the total view factor can then be calculated as:

$$F_{V-A_2} = F_{V_1-A_2} + F_{V_2-A_2} \tag{A1}$$

where

$$F_{V_1-A_2} = \frac{1}{\pi S}\tan^{-1}\left(\frac{h_1}{\sqrt{S^2-1}}\right) - \frac{h_1}{\pi S}\tan^{-1}\sqrt{\frac{S-1}{S+1}} + \frac{A_1 h_1}{\pi S\sqrt{A_1-1}}\tan^{-1}\sqrt{\frac{(S-1)(A_1+1)}{(S+1)(A_1-1)}} \tag{A2}$$

$$S = \frac{2R}{D} \tag{A3}$$

$$h_1 = \frac{2H_1}{D} \tag{A4}$$

$$A_1 = \frac{{h_1}^2 + S^2 + 1}{2S} \tag{A5}$$

$$F_{V_2-A_2} = \frac{1}{\pi S}\tan^{-1}\left(\frac{h_2}{\sqrt{S^2-1}}\right) - \frac{h_2}{\pi S}\tan^{-1}\sqrt{\frac{S-1}{S+1}} + \frac{A_2 h_2}{\pi S\sqrt{A_2-1}}\tan^{-1}\sqrt{\frac{(S-1)(A_2+1)}{(S+1)(A_2-1)}} \tag{A6}$$

$$h_2 = \frac{2H_2}{D} \tag{A7}$$

$$A_2 = \frac{{h_2}^2 + S^2 + 1}{2S} \tag{A8}$$

where A_2 is the area of target surface; R is the distance between the center of the pool fire and the target; H_1 is the distance between the target and the flame tip (as calculated from the flame height); H_2 is the distance of the target above the ground.

References

Ahmadi, O., Mortazavi, S.B., Pasdarshahri, H., Mahabadi, H.A., 2019a. Consequence analysis of large-scale pool fire in oil storage terminal based on computational fluid dynamic (CFD). Process Saf. Environ. 123, 379–389.

Ahmadi, O., Mortazavi, S.B., Pasdarshahri, H., Mahabadi, H.A., Sarvestani, K., 2019b. Modeling of boilover phenomenon consequences: computational fluid dynamics (CFD) and empirical correlations. Process Saf. Environ. 129, 25–39.

Broeckmann, B., Schecker, H.G., 1995. Heat transfer mechanisms and boilover in burning oil-water systems. J. Loss Prev. Proc. 8 (3), 137–147.

Chatris, J.M., Quintela, J., Folch, J., Planas, E., Arnaldos, J., Casal, J., 2001. Experimental study of burning rate in hydrocarbon pool fires. Combust. Flame 126 (1–2), 1373–1383.

Chen, J., Wang, D., Guo, L., Wang, Z., Kong, D., 2022. Experimental study on flame morphology and flame radiation of pool fire sheltered by plate obstacle. Process Saf. Environ. 159, 243–250.

Chen, Q., Liu, X., Wang, X., Zhao, J., Zhou, T., Ding, C., Wang, J., 2018. Experimental study of liquid fuel boilover behavior in normal and low pressures. Fire Mater. 42 (7), 843–858.

Ding, C., 2016. Experimental research on the flashpoint-boiling point of flammable liquid and their applications under low pressure. Hefei: University of Science and Technology of China.

Ding, L., Ji, J., 2023, Risk assessment and management of fire-induced domino effects in chemical industrial park, in Engineering Reliability and Risk Assessment, Ed. H Garg and M. Ram, 215–235.

Ding, L., Khan, F., Guo, X., Ji, J., 2021. A novel approach to reduce fire-induced domino effect risk by leveraging loading/unloading demands in chemical industrial parks. Process Saf. Environ. 146, 610–619.

Fan, W.C., Hua, J.S., Liao, G.X., 1995. Experimental study on the premonitory phenomena of boilover in liquid pool fires supported on water. J. Loss Prev. Proc. 8 (4), 221–227.

Ferrero, F., Muñoz, M., Kozanoglu, B., Casal, J., Arnaldos, J., 2006. Experimental study of thin-layer boilover in large-scale pool fires. J. Hazard Mater. 137 (3), 1293–1302.

Ferrero, F., Munoz, M., Arnaldos, J., 2007. Thin-layer boilover in diesel-oil fires: determining the increase of thermal hazards and safety distances. J. Hazard Mater. 140 (1–2), 361–368.

Garo, J.P., Vantelon, J.P., Fernandez-Pello, A.C., 1994. Boilover burning of oil spilled on water. in Symposium (International) on Combustion, Elsevier 25 (1), 1481–1488.

Hamins, A., Fischer, S.J., Kashiwagi, T., Kashiwagi, T., Klassen, M.E., Gore, J.P., 1994. Heat feedback to the fuel surface in pool fires. Combust. Sci. Technol. 97 (1–3), 37–62.

Hankinson, G., Lowesmith, B.J., 2012. A consideration of methods of determining the radiative characteristics of jet fires. Combust. Flame 159 (3), 1165–1177.

Heskestad, G., 1998. On Q* and the dynamics of turbulent diffusion flames. Fire Saf. J. 30 (3), 215–227.

Hu, L., Lu, K., Delichatsios, M., He, L., Tang, F., 2012. An experimental investigation and statistical characterization of intermittent flame ejecting behavior of enclosure fires with an opening. Combust. Flame 159 (3), 1178–1184.

Hu, X., He, Y., Li, Z., Wang, J., 2011. Combustion characteristics of n-heptane at high altitudes. P. Combust. Inst. 33 (2), 2607–2615.

Hua, R.S., 2011. Experimental study on combustion characteristics of methanol and ethanol pool fires under different low ambient pressure conditions. Hefei: University of Science and Technology of China.

Jiang, D., Pan, X.H., Hua, M., Mebarki, A., Jiang, J.C., 2019. Assessment of tanks vulnerability and domino effect analysis in chemical storage plants. J. Loss Prev. Proc. 60, 174–182.

Khan, F.I., Abbasi, S.A., 2001. An assessment of the likelihood of occurrence, and the damage potential of domino effect in a typical cluster of industries. J. Loss Prev. Process Ind. 14, 283–306.

Kong, D., Liu, P., Zhang, J., Fan, M., Tao, C., 2017. Small scale experiment study on the characteristics of boilover. J. Loss Prev. Proc. 48, 101–110.

Kong, D., Zhao, X., Chen, J., Yang, H., Du, J., 2021. Study on hazard characteristics and safety distance of small-scale boilover fire. Int. J. Therm. Sci. 164, 106888.

Koseki, H., Kokkala, M., Mulholland, G.W., 2006. Experimental study of boilover in crude oil fires. Fire Saf. Sci. 3, 865–874.

Laboureur, D., 2012. Experimental characterization and mondeling of hazards: BLEVE and Boilover. Engineering.

Laboureur, D., Aprin, L., Osmont, A., Buchlin, J.M., Rambaud, P., 2013. Small scale thin-layer boilover experiments: physical understanding and modeling of the water sub-layer boiling and the flame enlargement. J. Loss Prev. Proc. 26 (6), 1380–1389.

Li, Z., Zhang, P., 2021. Fire behaviors of fuels with different sootiness levels in hot and humid conditions. Process Saf. Environ. 146, 350–359.

Lin, X., 2017. Experiment on characteristics of small scale thin layer boilover. Hefei: University of Science and Technology of China.

Liu, C., Jangi, M., Ji, J., Yu, L., Ding, L., 2021. Experimental and numerical study of the effects of ullage height on plume flow and combustion characteristics of pool fires. Process Saf. Environ. 151, 208–221.

Ma, P., 2020. Study on influence of pressure and boiling point of water layer on boilover. Hefei: University of Science and Technology of China.

McGrattan, K.B., Baum, H.R., Hamins, A., 2000. Thermal radiation from large pool fires. Gaithersburg, MD, USA, J. Res. Natl. Inst. Stan. 35.

Mudan, K.S., 1984. Thermal radiation hazards from hydrocarbon pool fires. Prog. Energy Combust. Sci. 10.

Shaluf, I.M., Abdullah, S.A., 2011. Floating roof storage tank boilover. J. Loss Prev. Proc. 24 (1), 1–7.

Sudheer, S., Prabhu, S.V., 2010. Measurement of flame emissivity of gasoline pool fires. Nucl. Eng. Des. 240 (10), 3474–3480.

Sun, L., Cheng F., Wang J., 2022, Analysis and Prevention and Control System of Domino Accident Risk Data in Chemical Parks Based on Topological Neural Network, Computational Intelligence and Neuroscience, Article number 3712507.

Tauseef, S.M., Abbasi, T., Pompapathi, V., Abbasi, S.A., 2018. Case studies of 28 major accidents of fires/explosions in storage tank farms in the backdrop of available codes/standards/models for safely configuring such tank farms. Process Saf. Environ. 120, 331–338.

Vali, A., Nobes, D.S., Kostiuk, L.W., 2014. Transport phenomena within the liquid phase of a laboratory-scale circular methanol pool fire. Combust. Flame 161 (4), 1076–1084.

Wang, J., Yang, R., Tao, Z., Yang, W., Li, C., 2022. Experimental investigation on RP-3 aviation kerosene large-scale pool fires at high altitude. Fire Mater.

Zhao, J., Zhang, J., Chen, C., Huang, H., Yang, R., 2020. Experimental investigation on the burning behaviors of thin-layer transformer oil on a water layer. Process Saf. Environ. 139, 89–97.

Zhou, M., Xu, C., Xu, X., Li, X., 2023. Accident consequence assessment of benzene leakage from storage tank in a chemical park in Bengbu City, China. Process Saf. Prog. (in Press.).